RAA 2016 Vol. 16 No. 3, 47 (8pp) doi: 10.1088/1674–4527/16/3/047
http://www.raa-journal.org *http://iopscience.iop.org/raa*

Research in Astronomy and Astrophysics

Oxygen isotopic ratios toward molecular clouds in the Galactic disk

Hai-Kun Li[1,4], Jiang-Shui Zhang[1], Zhi-Wei Liu[1], Deng-Rong Lu[2], Min Wang[3] and Jin Wang[1]

[1] Center for Astrophysics, Guangzhou University, Guangzhou 510006, China; *jszhang@gzhu.edu.cn*
[2] Purple Mountain Observatory, Qinghai Station, Delingha 817000, China
[3] Purple Mountain Observatory, Chinese Academy of Sciences, Nanjing 210008, China
[4] School of Physics and Mechanical & Electrical Engineering, Xiamen University, Xiamen 361000, China

Received 2015 June 30; accepted 2015 October 27

Abstract We present our observations of the $J = 1 - 0$ rotation transitions in molecular isotopes C^{18}O and C^{17}O toward a sample of molecular clouds with different galactocentric distances, using the Delingha 13.7 m (DLH 13.7 m) telescope, administered by Purple Mountain Observatory, and its 9-beam SIS receiver. Complementary observations toward several sources with large galactocentric distance are obtained with the IRAM 30m and Mopra 22m telescopes. C^{18}O/C^{17}O abundance ratios reflecting the ^{18}O/^{17}O isotope ratios are obtained from integrated intensity ratios of C^{18}O and C^{17}O. We derived the ratio value for 13 sources covering a galactocentric distance range of 3 kpc to 16 kpc. In combination with our mapping results that provide a ratio value of 3.01±0.14 in the Galactic center region, it shows that the abundance ratio tends to increase with galactocentric distance, i.e., it supports a radial gradient along the Galactic disk for the abundance ratio. This is consistent with the inside-out formation scenario of our Galaxy. However, our results may suffer from small samples with large galactocentric distance. Combining our data with multi-transition lines of C^{18}O and C^{17}O will be helpful for constraining opacities and abundances and further confirming the Galactic radial gradient shown by the isotope ratio ^{18}O/^{17}O.

Key words: ISM: abundances — ISM: clouds — ISM: molecules — Galaxy: abundances — radio lines: ISM

1 INTRODUCTION

Isotope abundance ratios play a key role in our understanding of stellar nucleosynthesis, stellar ejecta and formation and chemical evolution of the Milky Way (e.g., Wilson & Rood 1994). The ^{18}O/^{17}O ratio is one of the most useful tracers of nuclear processing and metal enrichment. ^{18}O is believed to be primarily synthesized in massive stars ($M \geq 8M_{\odot}$) by helium burning, while ^{17}O should be dominantly ejected from longer-lived intermediate mass stars through carbon-nitrogen-oxygen (CNO) burning, with a longer production timescale (e.g., Henkel & Mauersberger 1993; Prantzos et al. 1996; Wouterloot et al. 2008). Thus the ^{18}O/^{17}O abundance ratio can reflect the relative number of massive stars compared to intermediate mass stars and further constrain the star-formation history of the Galaxy (Heikkilä et al. 1999).

The integrated line intensity ratio of C^{18}O/C^{17}O has been taken as a good measure of the ^{18}O/^{17}O abundance ratio (e.g., Zhang et al. 2007; Wouterloot et al. 2008). The main advantage is that the rotation transition lines of both molecules, which have similar chemical and excitation properties, are normally optically thin. Another advantage is that ^{18}O/^{17}O line ratios are small ($\ll$10) so that required sensitivities are not extremely different, when measuring one or the other CO subspecies. In addition, oxygen isotope fractionation does not have much affect on the molecular oxygen abundance ratios. The main reason is the high first ionization potential of oxygen, which causes low abundance of O^{+}. Thus the corresponding low level charge-molecular exchange reaction should cause few effects on the molecular oxygen abundance ratio (Langer et al. 1984; Wouterloot et al. 2008).

Similar works on the Galactic abundance ratio of ^{18}O/^{17}O have been performed mostly toward molecular clouds with small or moderate galactocentric distance, which reported the ratio ^{18}O/^{17}O to be around 4 (Wilson et al. 1981; Bensch et al. 2001; Ladd 2004; Wouterloot et al. 2005; Zhang et al. 2007). Toward the Galactic center region, single point observations were only performed for Sgr B2 and Sgr A and lower ratio values were reported (Penzias 1981; Guelin et al. 1982; Wouterloot et al. 2008). Penzias (1981) reported one uniform ratio value of ^{18}O/^{17}O around 3.5 from the molecular clouds in the Galactic center to sources with one galactocentric distance of 12 kpc. Wouterloot et al. (2008) determined the ratio ^{18}O/^{17}O across the entire Galaxy with galactocentric distance from 0.1 to 16.9 kpc, through observations of three transitions of C^{18}O and C^{17}O. Their analysis results proposed a gradient with increasing ^{18}O/^{17}O ratios as a function of the galactocentric distance, with average values of 2.88±0.11, 4.16±0.09 and 5.03±0.45 for Sgr B2 in the Galactic center, sources at 4–11 kpc and sources at > 16.5 kpc. respectively. However, their results suffer from small number statistics, especially for sources in the Galactic center and the outer Galaxy.

Believing that $C^{17}O$ has a longer formation timescale than $C^{18}O$ would be consistent with the decrease in the ratio $^{18}O/^{17}O$ with time (Wilson & Rood 1994). In this case, the ratio $^{18}O/^{17}O$ from the Galactic center region should be smaller than that from the Galactic disk and one radial gradient on $^{18}O/^{17}O$ should exist, adopting an inside-out scenario for the formation of our Galaxy. We are undertaking a systematic observational study on the ratio of ^{18}O to ^{17}O. This includes detailed mapping towards more molecular clouds in the Galactic center (Zhang et al. 2015) and single point observations toward disk molecular clouds with different galactocentric distances, especially more sources with large galactocentric distances, to check the existence of the ratio $^{18}O/^{17}O$ gradient along the Galactic disk (this work).

In Section 2, observations are described. Section 3 presents data reduction and analysis results, while discussion on the ratio is made in Section 4, and Section 5 summarizes the main results.

2 OBSERVATIONS

2.1 Delingha 13.7 m observations

On 2012 June 18 and December 4–11, we used the Delingha 13.7 m (DLH 13.7 m) telescope, administered by Purple Mountain Observatory (PMO), to observe the $J = 1 - 0$ lines of ^{12}CO, ^{13}CO, $C^{18}O$ and $C^{17}O$ toward 17 molecular clouds with different galactocentric distances, including seven sources with galactocentric distances larger than 11 kpc (Wouterloot & Brand 1989; Snell et al. 2002; Roman-Duval et al. 2009, see Table 1). A cryogenically cooled 9-beam (3×3) SIS receiver was used, with a separation of 174″ between the centers of adjacent beams. The full beam width to half power was ∼52″ and the pointing and tracking accuracies were estimated to be better than 9″. A fast Fourier transform spectrometer (FFTS) of 16 384 channels with a total bandwidth of 1 GHz was used for each beam, supplying a velocity resolution of about 0.21 km s^{-1}. The main-beam efficiency was about 0.48 at 110 GHz[1] and the main beam bright temperature scale was used here. Typical system temperature was around 150–300 K, depending on the weather conditions, with an average system temperature of 230 K. The position switch (PS) mode was adopted for single point observations.

2.2 Complementary Observations

Since $C^{18}O$ and $C^{17}O$ were only detected from a few sources with large galactocentric distances by our DLH 13.7 m observations, complementary observations (private communication) were made using IRAM 30m[2] and Mopra 22m[3].

Due to the large amount of noise in the spectra of IRAS 0245 taken from our DLH 13.7 m spectra, this target was also observed on 2014 July 7 through the IRAM 30m telescope. For the source IRAS 0245, its $C^{17}O$ $J = 1 - 0$ was not detected (due to large noise) by our DLH telescope observations. Thus this target was also observed through the IRAM 30m telescope with better sensitivity. The observations were carried out in position switching mode with the off position alternating between (−1800″, 0″) and (1800″, 0″) offset in R.A. and Dec. from the source and $C^{18}O$ and $C^{17}O$ lines were observed simultaneously with an integration time of about 40 minutes. The Eight Mixer Receiver (EMIR) was used, which provides a bandwidth of ∼8 GHz simultaneously in both polarizations per sideband. The FFTS backend was used, providing a frequency resolution of 195 kHz or velocity resolution of 0.53 km s^{-1} around 110 GHz. The main beam bright temperature could be obtained as the antenna temperature multiplied by the ratio of the forward efficiency to the main beam efficiency (∼0.95/0.77).

Another source with a galactocentric distance of 12.65 kpc, IRAS 07598 (Snell et al. 2002), was observed by the Mopra 22m on 2014 June 19. Its 3 mm receiver and MOPS spectrometer in Wideband Mode was used. It provides continuous coverage over 8.3 GHz using four overlapping sub-bands. Each sub-band is 2.2 GHz wide with 2×8096 channels, which corresponds to a velocity resolution of ∼0.4 km s^{-1} around 110 GHz. The main beam efficiency is around 0.42 (Ladd et al. 2005). A position switching mode was used and the typical system temperature was about 400 K. $C^{18}O$ and $C^{17}O$ lines were observed simultaneously, with an integration time of ∼30 minutes.

3 ANALYSIS & RESULTS

Our $C^{18}O$ and $C^{17}O$ $J = 1 - 0$ spectra were reduced by the software package GILDAS (e.g., Guilloteau & Lucas 2000). The individual spectra were subtracted with a first order polynomial fit to baselines. All DLH 13.7 m spectra were smoothed to a velocity resolution of about 0.66 km s^{-1} and that of our IRAM 30m and Mopra 22m spectra were 0.53 km s^{-1} and 0.7 km s^{-1}, respectively. Among our DLH 13.7 m observations, five of our seventeen sources, IRAS 02383, WB 440, WB 434, WB 529 and WB 793, have $C^{18}O$ spectra with low signal-to-noise ratio and the latter four were not observed with $C^{17}O$ (only IRAS 02383 was observed with very low signal-to-noise for $C^{17}O$.).

All DLH 13.7 m spectra are presented in Figure 1 and the IRAS 0245 spectra from IRAM 30m and IRAS 07598

[1] *http://www.dlh.pmo.cas.cn/hzjl/gjjldt/201012/t20101224_3049390.html*

[2] IRAM 30m is supported by INSU/CNRA (France), MPG (Germany) and IGN (Spain).

[3] Mopra 22m is part of the Australia Telescope National Facility which is funded by the Commonwealth of Australia for operation as a National Facility managed by CSIRO.

Table 1 $C^{18}O$ and $C^{17}O$ $J=1-0$ Observations in Our Sample

Source name	R.A. (J2000)	Dec. (J2000)	D_{GC} (kpc)	Line	Time (min)	rms (K)	ΔV (km s^{-1})
DLH 13.7 m							
G22.89+0.39	18:31:34.33	–08:44:50.7	3.3	$C^{18}O$	3	0.154	0.66
				$C^{17}O$	20	0.039	0.66
G24.39+0.04	18:35:37.39	–07:34:40.4	3.5	$C^{18}O$	35	0.248	0.66
				$C^{17}O$	10	0.045	0.66
G23.54	18:33:19.47	–08:14:24.7	4.2	$C^{18}O$	3	0.082	0.66
				$C^{17}O$	7	0.059	0.66
W33	18:14:14.39	–17:55:49.9	4.8	$C^{18}O$	21	0.122	0.66
				$C^{17}O$	10	0.049	0.66
G049.49	19:23:40.5	14:31:05.5	6.5	$C^{18}O$	3	0.094	0.66
				$C^{17}O$	5	0.053	0.66
G035.14	18:58:12.62	01:40:50.5	6.8	$C^{18}O$	3	0.063	0.66
				$C^{17}O$	5	0.062	0.66
G034.04–0.3	18:54:33.70	00:50:41.2	7.7	$C^{18}O$	3	0.084	0.66
				$C^{17}O$	10	0.043	0.66
DR 21OH	20:39:01.91	42:22:45.8	8.5	$C^{18}O$	21	0.069	0.66
				$C^{17}O$	10	0.034	0.66
NGC 2024	05:41:45.32	–01:54:47.2	8.9	$C^{18}O$	3	0.071	0.66
				$C^{17}O$	7	0.057	0.66
W3 OH	02:27:04.18	61:52:25.4	10	$C^{18}O$	3	0.060	0.66
				$C^{17}O$	7	0.046	0.66
IRAS 0245	02:45:12.36	60:49:45.4	14.3	$C^{18}O$	10	0.029	0.66
				$C^{17}O$	36	0.028	0.66
WB437	02:43:29.00	62:57:16.0	16.24	$C^{18}O$	12	0.031	0.66
				$C^{17}O$	60	0.016	0.66
IRAS 02383	02:42:20.09	62:53:51.7	16.24	$C^{18}O$	10	0.028	0.66
				$C^{17}O$	49	0.018	0.66
WB440	02:37:28.87	60:30:22.2	16.44	$C^{18}O$	16	0.025	0.66
WB434	02:41:29.36	60:43:14.7	17.91	$C^{18}O$	16	0.022	0.66
WB529	04:06:25.16	53:21:51.5	19.16	$C^{18}O$	12	0.031	0.66
WB793	06:22:01.80	15:18:06.8	19.30	$C^{18}O$	6	0.038	0.66
Mopra 22m							
IRAS 07598	08:01:54.82	–28:22:59.63	12.65	$C^{18}O$, $C^{17}O$	42	0.14	2.2
IRAM 30m							
IRAS 0245	02:45:12.40	60:49:45.0	14.3	$C^{18}O$, $C^{17}O$	30	0.016	1.5

spectra from Mopra 22m are presented in Figure 2. The Gaussian fitting results for those 14 sources (i.e., 12 sources from DLH 13.7 m, IRAS 0245 from IRAM 30 m and IRAS 07598 from Mopra 22m) are listed in Table 2, including the peak value ($T_{\rm peak}$), the line center velocity ($V_{\rm c}$), the line width (the full width at half maximum, FWHM) and the integrated intensity ($\int T_{mb} {\rm d}\nu$). The integrated intensity ratios of $C^{18}O$ and $C^{17}O$ can be calculated for these 14 sources. For WB 437 and IRAS 0245 observed by DLH 13.7 m and IRAS 07598 by Mopra 22m, the lower limits on the ratio can be just determined due to their $C^{17}O$ spectra having very low signal-to-noise ratio. To obtain the abundance ratio, the intensity ratio $C^{18}O/C^{17}O$ should be corrected from the frequency difference of both $J = 1-0$ lines, since $C^{18}O$ and $C^{17}O$ column densities are proportional to ν^{-2} times the integrated line intensity for clouds filling the beam (e.g., Linke et al. 1977). The abundance ratios can be derived through: $C^{18}O/C^{17}O$ (corrected)=$(\nu_{\rm C17O}/\nu_{\rm C18O})^2 C^{18}O/C^{17}O$ (observed). The intensity ratios and frequency-corrected ratios are also listed in Table 2.

Below we give comments on individual sources.

W33, G049.49, DR 21OH, NGC 2024, W3 OH and WB 437: Their ratios of $^{18}O/^{17}O$ were reported by previous observations (Penzias 1981; Wouterloot et al. 2008). For W33, DR 21OH, NGC 2024 and W3 OH, our derived intensity ratios are 3.73, 4.32, 3.88 and 4.72, respectively, which are consistent with previous results (3.77, 3.40, 3.89 and 3.11 from Penzias 1981; 3.98, 4.73, 3.79 and 3.87 from Wouterloot et al. 2008). G049.09 spectra show two velocity components around 50 km s^{-1} and 61 km s^{-1}, respectively. The derived abundance ratio for its two components are 3.89$\pm$0.17 and 4.43$\pm$0.07, which are in agreement with reported results from Wouterloot et al. (2008). For another source WB 437, the lower limit of the ratio by DLH 13.7 m is $\sim$5.42, which is consistent with a value of 5.86 reported by Wouterloot et al. (2008).

G 22.89+0.39, G 24.39+0.04, G 23.54, G 035.14, G 034.04–0.3, IRAS 0245 and IRAS 07598: No results of isotope ratio $^{18}O/^{17}O$ have been reported yet for these seven sources. For G 22.89+0.39, G 24.39+0.04, G 23.54 and G 035.14, their $C^{17}O$ spectra show possible features of hyperfine structure (hfs), which originates from the interaction of the electric quadrapole with the magnetic

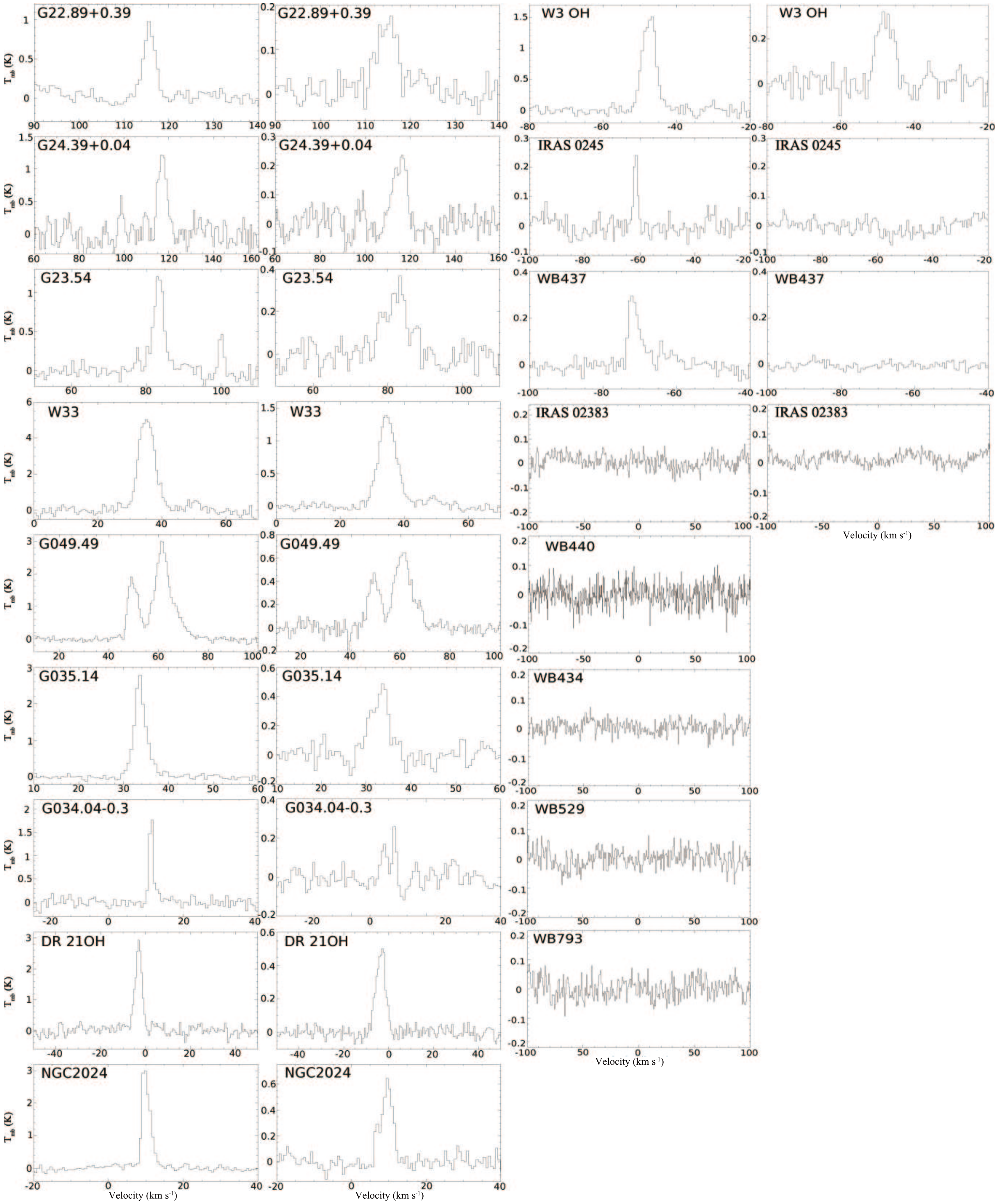

Fig. 1 C[18]O (*left panels*) and C[17]O (*right panels*) spectra for our sample, from observations with the DLH 13.7 m telescope. For WB 440, WB 434, WB 529 and WB 793, only their C[18]O spectra with low signal-to-noise are presented, since C[17]O was not observed in those cases.

dipole of C[17]O molecules (Frerking & Langer 1981). The hfs of C[17]O (1–0) has three hyperfine components and the maximum velocity separation between the hfs components is 3.26 km s^{-1} (Hofner et al. 2000). For these four sources, we have tried to fit the relative intensity of two C[17]O groups of hyperfine components. Due to the low spectral resolution, reliable results cannot be provided by a two-component fitting for G22.89+0.39, G24.39+0.04 and G23.54. For G035.14, two components can fit their spectra well and fitting results are comparable to those of a one component fitting. Thus one-component fitting results for these sources are taken for determining the

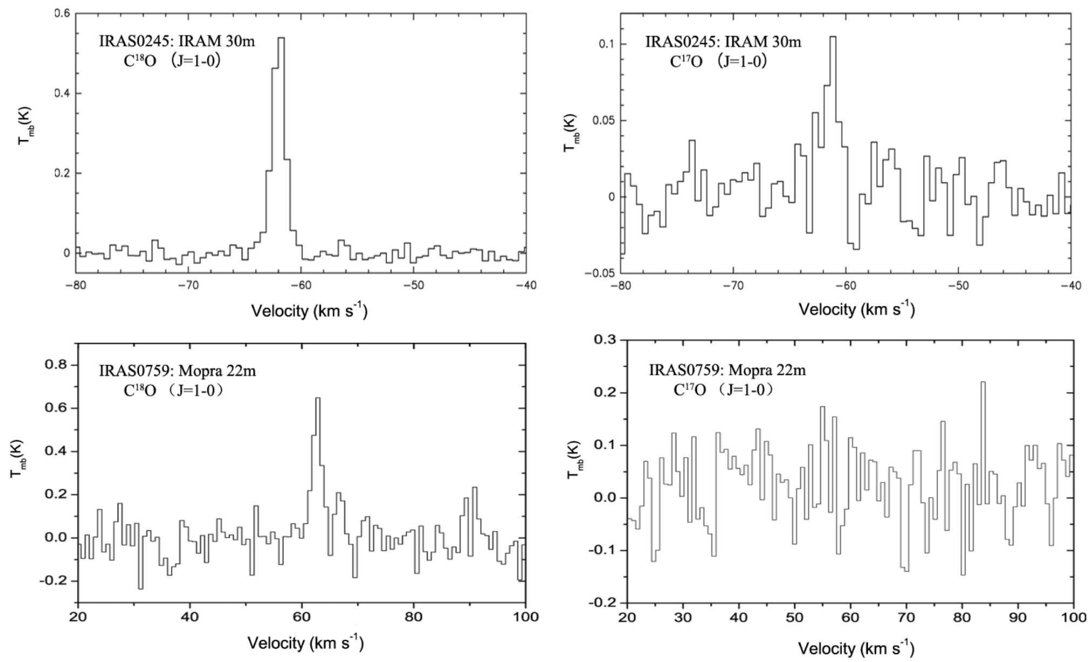

Fig. 2 Complementary observations of sources with large galactocentric distance through the Mopra 22m (IRAS 07598) and IRAM 30m telescopes (IRAS 0245).

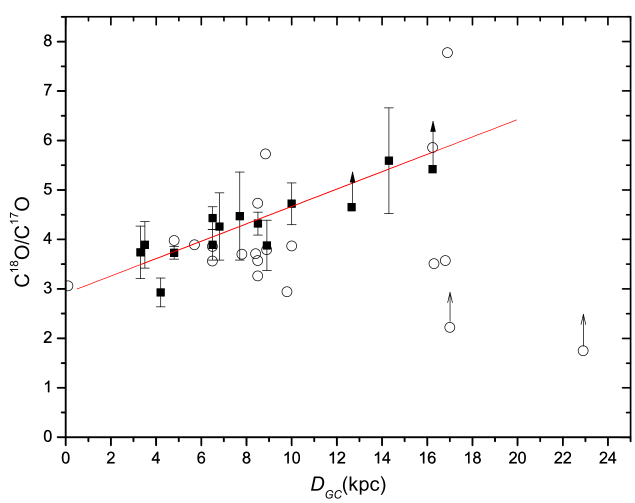

Fig. 3 C^{18}O/C^{17}O abundance ratios as a function of the galactocentric distance ($D_{\rm GC}$). The black squares show our new results and the empty circles represent the $J = 1-0$ line results from Wouterloot et al. (2008). The arrows indicate lower limits on the ratio for sources with low signal-to-ratio spectra for C^{17}O.

abundance ratio. For the source G034.04–0.3, its C^{17}O spectra show two velocity components around $\sim$9 km s^{-1} and $\sim$12 km s^{-1}, whereas its C^{18}O spectra only show a $\sim$12 km s^{-1} component. Its ^{13}CO spectra also only show this component. Thus, its intensity ratio C^{18}O/C^{17}O was determined for the 12 km s^{-1} component. For IRAS 0245, the lower limit on the abundance ratio ^{18}O/^{17}O by DLH 13.7 m is $\sim$5.48, which is supported by the result from complementary IRAM 30m observations, with a ratio of 5.59$\pm$1.07. For another source, IRAS 07598, only the lower limit of the ratio can be obtained with a value of $\sim$4.65, through its estimated C^{17}O integrated intensity (by its root mean square (rms) value$\times$FWHM, assuming the same FWHM value as its C^{18}O).

4 DISCUSSION

As mentioned in Section 1, Wouterloot et al. (2008) reported a possible gradient with increasing ^{18}O/^{17}O as a function of the galactocentric distance, rising from $\sim$3.0 in the Galactic center (specifically Sgr B2) to $\sim$5.0 in the outer arm of the Galactic disk at $D_{\rm GC}\sim$16 kpc. Our ^{18}O/^{17}O ratio results are plotted as a function of the galactocentric distance in Figure 3 (black squares). For comparison, results from Wouterloot et al. (2008) are also

Table 2 Measured Galactic Values of ^{18}O/^{17}O

Source name	$T_{\rm peak}$		$V_{\rm c}$		Width		$\int T_{mb} {\rm d}\nu$		R	R_f
	(C^{18}O)	(C^{17}O)	(C^{18}O)	(C^{17}O)	(C^{18}O)	(C^{17}O)	(C^{18}O)	(C^{17}O)	C^{18}O/C^{17}O	
	(K)		(km s^{-1})		(km s^{-1})		(K km s^{-1})			
(1)	(2)	(3)	(4)	(5)	(6)	(7)	(8)	(9)	(10)	(11)
G22.89+0.39	0.93	0.16	115.7	114.8	3.00	5.35	3.07(0.15)	0.86(0.08)	3.57(0.51)	3.74(0.53)
G24.39+0.04	1.25	0.23	117.05	115.38	4.58	6.62	6.07(0.29)	1.63(0.12)	3.72(0.45)	3.89(0.47)
G23.54	1.22	0.33	83.3	83.0	3.47	4.65	4.51(0.26)	1.61(0.07)	2.80(0.28)	2.93(0.29)
W33	5.24	1.39	35.2	34.7	6.02	6.43	33.63(0.56)	9.44(0.17)	3.56(0.12)	3.73(0.13)
G049.49	1.84	0.45	49.7	49.2	4.69	5.13	9.16(0.17)	2.46(0.15)	3.72(0.30)	3.89(0.31)
	2.65	0.63	61.7	60.9	8.01	8.38	23.65(0.44)	5.59(0.19)	4.23(0.22)	4.43(0.23)
G035.14	2.54	0.57	33.6	33.7	3.04	5.04	8.24(0.14)	2.02(0.29)	4.07(0.65)	4.26(0.68)
G034.04–0.3	1.77	0.14	11.46	9.93	1.24	4.05	2.65(0.14)	0.62(0.09)	4.27(0.85)	4.47(0.89)
DR 21OH	2.93	0.50	–3.14	–3.51	3.47	4.95	10.81(0.20)	2.62(0.09)	4.13(0.22)	4.32(0.23)
NGC 2024	3.05	0.69	10.06	9.95	2.67	3.18	8.68(0.21)	2.34(0.25)	3.71(0.49)	3.88(0.51)
W3 OH	1.54	0.30	–47.5	–47.9	4.31	4.92	7.08(0.14)	1.57(0.11)	4.51(0.41)	4.72(0.42)
IRAS07598 (Mopra 22m)	0.51	0.11	62.9	*	2.78	*	1.42(0.2)	$\leq$0.32	$\geq$4.44	$\geq$4.65
IRAS0245 (DLH 13.7m)	0.26	0.05	–61.5	*	1.56	*	0.44(0.04)	$\leq$0.084	$\geq$5.24	$\geq$5.48
IRAS0245 (IRAM 30m)	0.56	0.09	–62.0	–61.3	1.41	1.57	0.833(0.02)	0.156(0.026)	5.34(1.02)	5.59(1.07)
WB437	0.28	0.05	–71.7	*	2.93	*	0.88(0.02)	$\leq$0.17	$\geq$5.18	$\geq$5.42

Notes: Column (1): source name; Columns (2) and (3) the peak values of C^{18}O and C^{17}O respectively; Columns (4) and (5): the line center velocity of C^{18}O and C^{17}O lines respectively; Columns (6) and (7): the line width of C^{18}O and C^{17}O lines respectively; Columns (8) and (9): the integrated line intensity of C^{18}O and C^{17}O respectively; Column (10): the intensity ratio C^{18}O/C^{17}O. Column (11): the frequency-corrected ratios.

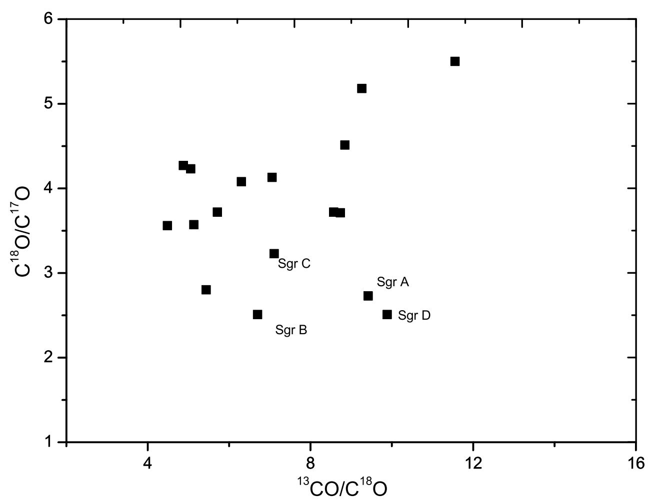

Fig. 4 The C^{18}O/C^{17}O abundance ratio versus the ^{13}CO/C^{18}O relative line intensity for our sample (*squares*). For comparison, results from the Galactic center region are also presented, including Sgr A, Sgr B, Sgr C and Sgr D, taken from Zhang et al. (2015).

presented in Figure 3 (empty circles). The trend is obvious, i.e., the ratio ^{18}O/^{17}O increases with galactocentric distance. To compare with results of Wouterloot et al. (2008), the average ratio for two groups was derived. It is 4.35$\pm$0.45 and >5.27 for sources at 3 kpc<$D_{\rm GC}$<11 kpc and $D_{\rm GC}$>11 kpc, respectively which is consistent with their results. Combining with our mapping results that provide a ratio value of 3.01$\pm$0.14 in the Galactic center region (Zhang et al. 2015), a linear least-squares fit gives ^{18}O/^{17}O=(0.18$\pm$0.04)$D_{\rm GC}$+(2.91$\pm$0.27), with a Spearman's rank correlation coefficient $R = 0.85$. However, we have to note that our sources with galactocentric distance larger than 11 kpc are still not enough, and the $J = 1-0$ transitions alone (C^{18}O and C^{17}O) are not sufficient when trying to account for radiative transfer effects. Our proposed observations of C^{18}O and C^{17}O

$J = 2-1$ and $J = 3-2$ lines using the James Clerk Maxwell Telescope (JCMT) and/or the Caltech Submillimeter Observatory (CSO) would be important for constraining opacities and abundances in our sources and further verifying this Galactic radial gradient of the isotope ratio ^{18}O/^{17}O.

Generally, the molecular isotopologue ratios derived from the molecular line intensity should consider possible effects from optical depth, chemical fractionation or selective photodissociation. For our results on the ^{18}O/^{17}O isotope ratio determined from the line intensity ratio C^{18}O/C^{17}O, the fractionation of oxygen is negligible due to its high first ionization potential (see details in Sect. 1, also Langer et al. 1984). The C^{17}O line is optically thin and the C^{18}O is also normally optically thin. However, under extreme conditions with large optical depth, saturation of C^{18}O lines could lead to underestimating the real isotope ratio of ^{18}O/^{17}O. Isotope selective photodissociation (more self-shielding from C^{18}O) could increase the ^{18}O/^{17}O ratio. The optical depth can be estimated directly for those sources with hfs features in C^{17}O spectra, through fitting the relative intensity of the two C^{17}O groups of hyperfine components. As mentioned in Section 3, there are four sources with possible hfs features. However, only G 035.14 can be fitted well with two components and it provides the optical depth of the C^{17}O $J = 1-0$ line of $<$0.02 and corresponding value of $<$0.1 for the C^{18}O line, assuming τ[C^{18}O $J = 1-0$]$\sim$4τ[C^{17}O $J = 1-0$] (Wouterloot et al. 2008). Wouterloot et al. (2005) carried out observation and modeling studies on the interstellar C^{18}O/C^{17}O ratio towards the nearby low-mass star forming cloud ρ Oph and found that the effect of optical depth has to be considered for a few positions with C^{18}O column density $>1.0\times10^{16}$ cm^{-2}. Among our sample, W 33, which shows the largest integrated intensity, was reported with a peak ^{13}CO column density of 1.0×10^{17} cm^{-2} (Goldsmith & Mao 1983). This corresponds to a C^{18}O column density of $\sim10^{16}$ cm^{-2}, assuming a ratio ^{13}CO/C^{18}O $\sim$ 10 (Zhang et al. 2007). Thus, the effect of optical depth should not have much influence on our results. This is supported by the plot of the integrated intensity ratio C^{18}O/C^{17}O versus ^{13}CO/C^{18}O (Fig. 4), which shows that C^{18}O/C^{17}O appears to be independent of ^{13}CO/C^{18}O. One would expect any diminution in C^{18}O/C^{17}O due to line saturation to be the most apparent in sources having the most saturated ^{13}CO lines (Penzias 1981).

5 SUMMARY AND PROSPECTS

To investigate the oxygen isotope ratio of ^{18}O/^{17}O across the entire Galaxy, we acquired Delingha 13.7 m observations in the C^{18}O and C^{17}O $J = 1-0$ lines toward a sample of molecular clouds with different galactocentric distances. Complementary observations by the IRAM 30m and Mopra 22 m telescopes were also used. The C^{18}O/C^{17}O ratio reflecting the ^{18}O/^{17}O isotope ratio are obtained from the integrated intensity ratios of C^{18}O and C^{17}O lines for our 13 sources. For sources from the Galactic disk with a galactocentric distance of 3–11 kpc, ^{18}O/^{17}O = 4.35$\pm$0.45 and for sources with galactocentric distance larger than 11 kpc, ^{18}O/^{17}O$>$5.27. In combination with our mapping results that provide a ratio value of 3.01$\pm$0.14 toward the Galactic center region, a ^{18}O/^{17}O gradient along the galactic disk is apparent, with a linear fit of ^{18}O/^{17}O=(0.2$\pm$0.1)$D_{\rm GC}$+(3.0$\pm$0.5). This gradient is consistent with the inside-out formation scenario for our Galaxy. However, only one source with $D_{\rm GC}$$>$11 kpc is obtained with a reliable ratio ^{18}O/^{17}O. More sources with large galactocentric distance are needed in order to confirm the ^{18}O/^{17}O radial gradient. In addition, we only observed $J = 1-0$ lines of C^{18}O and C^{17}O and the $J = 1-0$ lines alone are not sufficient when trying to account for radiative transfer effects. Future observations of the $J = 2-1$ and $J = 3-2$ transitions of C^{18}O and C^{17}O using the JCMT and/or CSO telescope would be important for constraining opacities and abundances and further verifying this Galactic radial gradient for ^{18}O/^{17}O.

Acknowledgements This work is supported by the National Basic Research Program of China (973 program, 2012CB821800) and the National Natural Science Foundation of China (Nos. 11178009 and 11473007). We would like to thank the staff at Qinghai Station of PMO for their assistance during our observations and thank the Key Laboratory for Radio Astronomy, Chinese Academy of Sciences for partly supporting the operation of the DLH 13.7 m telescope. Many thanks go to Dr. C. Henkel and Y. Zhang for their help on the IRAM 30m and Mopra 22m observations. We make use of the NASA Astrophysics Data System Bibliographic Services (ADS) and also the NASA/IPAC Extragalactic Database (NED), which is operated by the Jet Propulsion Laboratory.

References

Bensch, F., Pak, I., Wouterloot, J. G. A., Klapper, G., & Winnewisser, G. 2001, ApJ, 562, L185

Frerking, M. A., & Langer, W. D. 1981, J. Chem. Phys., 74, 6990

Goldsmith, P. F., & Mao, X.-J. 1983, ApJ, 265, 791

Guelin, M., Cernicharo, J., & Linke, R. A. 1982, ApJ, 263, L89

Guilloteau, S., & Lucas, R. 2000, in Astronomical Society of the Pacific Conference Series, 217, Imaging at Radio through Submillimeter Wavelengths, eds. J. G. Mangum, & S. J. E. Radford, 299

Heikkilä, A., Johansson, L. E. B., & Olofsson, H. 1999, in IAU Symposium, 190, New Views of the Magellanic Clouds, ed. Y.-H. Chu, N. Suntzeff, J. Hesser, & D. Bohlender, 275

Henkel, C., & Mauersberger, R. 1993, A&A, 274, 730

Hofner, P., Wyrowski, F., Walmsley, C. M., & Churchwell, E. 2000, ApJ, 536, 393

Ladd, E. F. 2004, ApJ, 610, 320

Ladd, N., Purcell, C., Wong, T., & Robertson, S. 2005, PASA, 22, 62

Langer, W. D., Graedel, T. E., Frerking, M. A., & Armentrout, P. B. 1984, ApJ, 277, 581

Linke, R. A., Goldsmith, P. F., Wannier, P. G., Wilson, R. W., & Penzias, A. A. 1977, ApJ, 214, 50
Penzias, A. A. 1981, ApJ, 249, 518
Prantzos, N., Aubert, O., & Audouze, J. 1996, A&A, 309, 760
Roman-Duval, J., Jackson, J. M., Heyer, M., et al. 2009, ApJ, 699, 1153
Snell, R. L., Carpenter, J. M., & Heyer, M. H. 2002, ApJ, 578, 229
Wilson, R. W., Langer, W. D., & Goldsmith, P. F. 1981, ApJ, 243, L47
Wilson, T. L., & Rood, R. 1994, ARA&A, 32, 191
Wouterloot, J. G. A., & Brand, J. 1989, A&AS, 80, 149
Wouterloot, J. G. A., Brand, J., & Henkel, C. 2005, A&A, 430, 549
Wouterloot, J. G. A., Henkel, C., Brand, J., & Davis, G. R. 2008, A&A, 487, 237
Zhang, J. S., Henkel, C., Mauersberger, R., et al. 2007, A&A, 465, 887
Zhang, J. S., Sun, L. L., Riquelme, D., et al. 2015, ApJS, 219, 28